Dual Boost-Driven Graph-Level Clustering Network

John Smith *, Wenxuan Tu * ¶, Junlong Wu *, Wenxin Zhang †, Jingxin Liu *, Haotian Wang *,
Jieren Cheng *‡, Huajie Lei *, Guangzhen Yao ‡, Lingren Wang *, Mengfei Li *, Renda Han ‡ and Yu Li†
*University of Chinese Academy of Science, Beijing, China
†Northeast Normal University, Changchun, China
‡Hubei University, Wuhan, China
¶Corresponding Author. Email: rmrb_send@163.com

***Abstract*—Graph-level clustering remains a pivotal yet formidable challenge in graph learning. Recently, the integration of deep learning with representation learning has demonstrated notable advancements, yielding performance enhancements to a certain degree. However, existing methods suffer from at least one of the following issues: 1) the original graph structure has noise, and 2) during feature propagation and pooling processes, noise is gradually aggregated into the graph-level embeddings through information propagation. Consequently, these two limitations mask clustering-friendly information, leading to suboptimal graph-level clustering performance. To this end, we propose a novel Dual Boost-Driven Graph-Level Clustering Network (DBGCN) to alternately promote graph-level clustering and filtering out interference information in a unified framework. Specifically, in the pooling step, we evaluate the contribution of features at the global level and optimize them using a learnable transformation matrix to obtain high-quality graph-level representation, such that the model's reasoning capability can be improved. Moreover, to enable reliable graph-level clustering, we first identify and suppress information detrimental to clustering by evaluating similarities between graph-level representations, providing more accurate guidance for multi-view fusion. Extensive experiments demonstrated that DBGCN outperforms the state-of-the-art graph-level clustering methods on six benchmark datasets.**

***Index Terms*—Graph-level Clustering, Deep Graph Clustering, Graph Neural Network, Unsupervised Learning.**

I. Introduction

Graph-level clustering is a crucial task in the field of machine learning, focused on grouping multiple graphs without labels into distinct clusters. Meanwhile, the ubiquity of graph structures has led to the widespread application of graph-level clustering methods across various domains. For example, in voice processing, graph-level clustering plays a significant role in multiple tasks such as speaker recognition, speech synthesis, and emotion detection [1]–[3]. In medical data analysis, it has proven valuable for phenotype classification, disease diagnosis, and predicting patient outcomes [4]–[6]. Similarly, in chemical molecular modeling, graph-based techniques are employed to represent molecular structures, predict chemical properties, and discover novel compounds with targeted characteristics [7], [8]. These universal applications further emphasize the pivotal role of graph-level clustering in advancing progress and innovation across these key domains. Existing methods guide the clustering process by refining the low-dimensional embeddings of each graph, thus enhancing the quality of representations. However, the inherent structural diversity and dynamic nature of graphs have shifted the focus, complicating the process and increasing the difficulty of feature extraction.

Over the past years, traditional methods e.g., spectral clustering [9] and subspace clustering [10], have played a dominant role. With the emergence of Graph Neural Networks (GNNs), the representation learning ability in the latent space of deep learning has injected new vitality into graph-level clustering tasks. Nonetheless, research on graph-level clustering remains limited. The main idea of most existing deep learning approaches primarily generates node-level embeddings through GNNs, which are subsequently pooled to obtain discriminative graph-level embeddings. For instance, Representing graphs via Gromov-Wasserstein factorization (GWF) [11] captures structural similarities between graphs by comparing their distributions in a metric space to align graphs of varying sizes and structures. However, GWF faces challenges when applied to noisy graphs or those with incomplete structure information, as the factorization process may not fully capture the underlying graph structure. To alleviate this issue, Graph-Level Clustering Framework (GLCC) [12] constructs an adaptive similarity matrix to probe instance- and cluster-level contrastive learning (CL) to generate clustering-friendly embeddings. However, the reliance on hyperparameter tuning and neighbor-aware pseudo-labels could introduce sensitivity to noisy or imbalanced data. Similarly, UDGC [13] enforces a uniform distribution of instances across clusters and scatters these clusters on a unit hypersphere to improve cluster-level separation, addressing issues of insufficient representation discriminability. Moreover, DGLC [14] partitions graphs into groups based on similarity, learning discriminative graph-level embedding by maximizing the mutual information between graphs and their substructures. This approach is further regularized to generate pseudo-labels, ensuring the discriminability of the learned representations.

Despite recent advances in design and theory, current graph-level clustering methods still face challenges when handling highly noisy and heterogeneous data. While effective for node-level clustering, these representations that rely on visible information windows suffer from repeated amplification of noise during graph-level pooling, failing to capture broader information and leading to chaotic and diminished graph-level representations. Furthermore, node-level pooling often fails to

prioritize important information, instead amplifying irrelevant features. The lack of effective optimization mechanisms for the dynamic nature of graphs further reduces the accuracy of graph-level representations, which further limits clustering performance.

To address these issues, we propose a network termed DBGCN, which comprises two modules: a Multi-view Contrast Fusion Scheme (MCFS) and a Learnable Hierarchical Pooling Mechanism (LHPM). The former introduces multi-view contrast optimization and dynamic information fusion, which filter out sub-optimal and noisy information at node and graph levels to generate distinctive feature embedding in high-dimensional space. The latter, utilizing hierarchical feature alignment to effectively suppress noise, gradually refines context structure information and produces enriched graph-level representations, which facilitates clustering performance. These two modules promote each other through iterative optimization enhancing the compactness of clustering. In summary, our contributions are as follows.

- A novel fusion network for graph-level clustering is designed, which effectively extracts high-confidence graph-level features to generate a robust cluster distribution.
- The contrastive fusion scheme leveraging multi-view learning refines high-dimensional features through multi-level similarity matrices while efficiently capturing both subspace and global information to construct graph-level representations.
- A hierarchical pooling mechanism identifies and infers key node features to enhance while filtering noise. This awareness process occurs in layers, progressively refining node representations to retain only the most relevant features to capture high-response graph-level patterns.
- Extensive experiments on six datasets show that our method outperforms the state-of-the-art.

II. Related Work

A. Node-level Feature Pool Method

In graph-level representation learning research, the design of pooling methods is crucial for extracting features. The pooling process serves as a sampling mechanism, aiming to compress node-level features into graph-level representations, which need to be discriminative of clusters while maintaining the unique characteristics of the nodes. In the early years, pooling operations were mainly performed through simple aggregation methods, such as maximum pooling, addition pooling, and average pooling [15]. These methods have been widely used for their intuitiveness and efficiency. Recently researchers have adopted attention mechanisms [16], [17] and multi-scale pooling methods [18] to improve performance. Particularly, Top-K computes an importance score for each node and dynamically selects the top K nodes with the highest scores for feature aggregation, generating graph-level embeddings. However, it potentially discards useful information from low-scoring nodes and is sensitive to the choice of the hyperparameter, which requires careful tuning for specific tasks [19]. Moreover, [20] proposed the diffpool method, which learns a differentiable soft assignment distribution for nodes at each GNN layer, mapping nodes to aggregate node embeddings into graph representations. [21] introduce a structure pooling method, capturing multi-scale structure information to enhance clustering performance. However, these methods rely on fixed strategies and are unable to adapt to the diverse and complex structures of graphs. Furthermore, they are not specifically designed for graph-level clustering, leading to suboptimal performance in such tasks. Consequently, improving graph-level clustering pooling methods has emerged as a critical and urgent challenge.

B. Deep Graph Clustering

Deep Clustering is a fundamental task in machine learning. Recently, GNN has significantly advanced deep node-level graph clustering. For instance, [22] proposed an auto-encoder (AE) to learn effective node features for clustering. However, this approach fails to exploit the unique advantages provided by structural information. To this end, [23] combined GCN and AE to learn node features for graph clustering, which provides broader insights into fully leveraging multi-source information in graphs. Moreover, DFCN [24] proposes a triplet self-supervised strategy for reliable cluster assignment. Methods based on Graph Contrastive Learning (GCL) have also received considerable attention. For instance, DAEGC [25] employed attention mechanisms to refine embeddings, while DGLC [26] explore dual-view representations to mitigate representation degeneration and improve clustering robustness. In terms of graph-level clustering, GLCC [12] combined neighborhood information to optimize clustering performance further. [13] attempted to address the issue of insufficient discriminability in graph-level representations by learning distributed cluster centers on the hypersphere. Moreover, DGLC [14] groups graphs based on similarity and enhances graph-level embedding by maximizing the relation information between the graphs and their substructures. Despite advancements in node clustering, graph-level clustering remains a significant research gap due to the complexity of measuring relationships between graphs.

III. Method

In this section, we first introduce the concepts and definitions of symbols, and then explain our proposed method in detail. The overall system architecture is shown in Fig. 1.

A dual-network architecture called DBGCN, consisting of the Graph Isomorphism Network (GIN) [27] and GCN, focuses on node attributes and graph structure features respectively to effectively extract subspaces and global structures. Specifically, we expand the window width of the GCN to capture high-dimensional structure features. Integrating with the attributes features achieves multi-view consensus. Additionally, we filter out graph-level low-yield features through comparison to refine the overall feature.

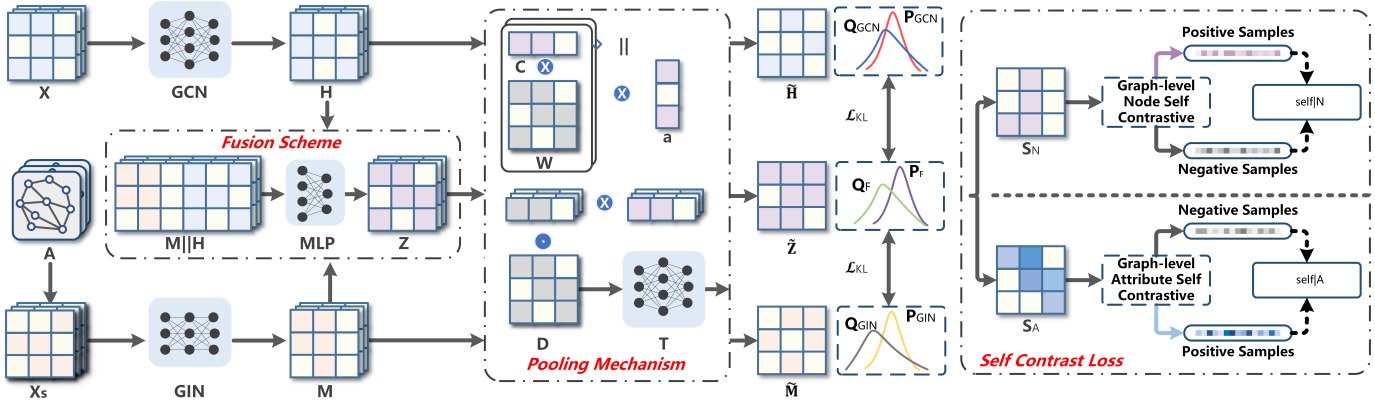

Fig. 1: The framework of DBGCN.

Algorithm 1 Training process of DBGCN

Require: Input data: $\mathbf{X}$, Graph: $\mathcal{G}$, Number of clusters: K.
Ensure: Clustering results $\mathbf{R}$.

```
Initialize W_gcn^(l), W_gin^(l) randomly;
for iter = 1 to MaxIter do
    Generate final embeddings H, M by GCN and GIN
    by Eq. (1)-(2);
    Fuse H and M to generate Z;
    Pool H, M, and Z to obtain graph-level embedding
    H̃, M̃, and Z̃ by Eq. (3)-(5);
    Generate Q and P distributions by H̃, M̃, and Z̃;
    Calculate self contract loss L_self and KL loss L_KL
    by Eq. (6)-(10);
    Backpropagate and update parameters;
end for
Calculate the clustering results by final embedding Z̃_f;
Return R
```

A. Notations

Given a set of N_G graphs $\mathcal{G} = \{G_1, G_2, ..., G_{N_G}\}$, where the i-th graph is $G_i = \{V_i, E_i\}$. Assume the graph has N nodes and d features per node. Its original adjacency matrix $\mathbf{A} \in \mathbb{R}^{N\times N}$ with self-loops is $\widetilde{\mathbf{A}} = \mathbf{A} + \mathbf{I}_N$. Its normalized degree matrix is $\widetilde{\mathbf{D}} \in \mathbb{R}^{N\times N}$. Its node attribute matrix is $\mathbf{X} \in \mathbb{R}^{N\times d}$. $\mathbf{X}_s \in \mathbb{R}^{N\times d}$ denotes the graph structure feature matrix.

B. GCN and GIN Networks

In the field of GNN, the GCN and GIN are prominent architectures designed for processing graph structure data. The forward propagation in GCN is defined by

$$\mathbf{H}^{(l+1)} = \sigma(\widetilde{\mathbf{D}}^{-\frac{1}{2}}\widetilde{\mathbf{A}}\widetilde{\mathbf{D}}^{-\frac{1}{2}}\mathbf{H}^{(l)}\overline{\mathbf{W}}^{(l)}), \tag{1}$$

where $\mathbf{H}^{(l)}$ is the l-th layer feature embedding matrix, $\overline{\mathbf{W}}^{(l)}$ is the l-th layer parameters matrix, σ is the activation function. In addition, GIN's update rule is given by

$$\mathbf{M}^{(l+1)} = \mathrm{MLP}^{(l+1)}\big((1+\varepsilon)\cdot\mathbf{M}^{(l)} + \widetilde{\mathbf{A}}\mathbf{M}^{(l)}\big), \tag{2}$$

where $\mathbf{M}^{(l)}$ represents the feature matrix at the l-th layer, and MLP [28] is a multi-layer perceptron. Based on this, the GIN encoder extracts the features of the original attribute $\mathbf{X}$ to obtain the final attribute potential representation $\mathbf{M}$. The GCN encoder extracts the graph structure features $\mathbf{X}_s$ that is generated by random walk [29] to obtain the final structure potential representation $\mathbf{H}$. Then, we concatenate the $\mathbf{H}$ and $\mathbf{M}$ to generate a fused final representation as $\mathbf{Z} = \mathrm{MLP}(\mathbf{H}||\mathbf{M})$. The fusion of GCN and GIN leverages the complementary strengths of both architectures to improve graph representation learning. GCN excels at capturing graph structure through convolution operations on the normalized adjacency and degree matrices, effectively encoding the relationships between nodes based on their connectivity. In contrast, GIN focuses on extracting node-level features by using an MLP with a residual connection, allowing it to model complex non-linear relationships between node attributes. In this way, the model benefits from both global graph structure and local node attributes.

C. Learnable Hierarchical Pooling Mechanism

Traditional pooling methods fail to adapt to diverse and complex graph structures. Traditional pooling methods struggle with complex graph structures due to their reliance on fixed strategies that neglect structural information, fail to capture higher-order dependencies, and lack the flexibility to handle heterogeneous graphs. To address these limitations, we propose the LHPM that dynamically adjusts to the input graph's features, effectively aggregating node representations into a more informative graph-level representation while preserving critical information and discarding irrelevant features. It employs a hierarchical refinement strategy that begins with coarse node aggregation and iteratively enhances the graph-level representation by capturing higher-order interactions. Additionally, a context-aware aggregation mechanism adapts the pooling process to the structural characteristics of the graph, improving adaptability and robustness.

Specifically, we enhance the node-level features $\mathbf{C}$ by assigning a quantitative importance score ω that is computed

as:

$$\omega_i = \text{Softmax}\big(\sigma(\sum_{j\in\mathcal{N}(i)} \mathbf{a}^\top \cdot [\mathbf{W}\mathbf{C}_i \| \mathbf{W}\mathbf{C}_j])\big) \text{ s.t. } i \neq j. \quad (3)$$

For each node i based on its local and global context. Where $\mathbf{a}$ and $\mathbf{W} \in \mathbb{R}^{d\times d'}$ are a weight vector and a learnable matrix, respectively. Then, the model adapts node selection by aggregating weighted node features to obtain a preliminary graph-level representation $\mathbf{C}_{graph|k}$ of the k-th graph as:

$$\mathbf{C}_{\text{graph|k}} = \frac{1}{N}\sum_{i=1}^{N} w_i \cdot \mathbf{C}_i \text{ s.t. } i \in \mathcal{G}_k \quad (4)$$

which is refined through a series of iterative layers that capture higher-order interactions and dependencies.

Hierarchical Refinement We use a dynamic feature transformation mechanism that adapts the feature space based on local graph properties, enhancing the ability to capture complex interactions, as:

$$\mathbf{C}^{(k)}_{\text{refined}} = \sigma\big(\mathbf{T}^{(k)}(\mathbf{C}^{(k-1)}_{\text{selected}} \odot \hat{\mathbf{D}}^{(k)}) + \mathbf{b}^{(k)}\big), \quad (5)$$

where $\mathbf{T}^{(k)} \in \mathbb{R}^{d\times d}$ is a dynamic transformation matrix learned for the k-th refinement layer, adapting based on the features and their interactions. $\odot$ represents Hadamard product. $\hat{\mathbf{D}}^{(k)}$ is a learnable matrix that adjusts the contribution of different features dynamically based on their relevance in the current context. $\mathbf{b}^{(k)}$ is a bias term for the k-th refinement layer. The refinement process is enhanced through three key mechanisms: i) $\mathbf{T}^{(k)}$ adapts to the feature space at each stage, enabling the model to capture complex interactions; ii) $\odot$ with a learnable matrix $\hat{\mathbf{D}}^{(k)}$ modulates feature influence based on their relevance; and iii) $\hat{\mathbf{D}}^{(k)}$ dynamically adjusts feature contributions, tailoring the refinement to the specific characteristics of the data. Finally, we generate the final graph-level representations $\widetilde{\mathbf{C}} = \mathbf{C}^{(K)}_{\text{refined}}$. The mechanism approach significantly enhances the model's ability to generalize across diverse graph types and complexities, adapting to variations in graph size, density, and structure.

D. Graph-level Contrast Learning

To effectively extract high-quality information for generating more compact and clustering-sensitive graph-level embeddings, we highly purify the graph-level fusion features $\widetilde{\mathbf{Z}}$ pooled by LHPM, by minimizing the contrast loss. This process includes graph-level node contrast optimization and graph-level attribute contrast optimization. Specifically, in the stage of graph-level attribute contrast optimization, we calculate graph-level attribute correlation matrix $\mathbf{S}_A$ as:

$$\mathbf{S}_A = \frac{(\widetilde{\mathbf{Z}})(\widetilde{\mathbf{Z}})^\top}{||\widetilde{\mathbf{Z}}||^2}. \quad (6)$$

Then, we minimize the graph-level attribute self contrast loss $\mathcal{L}_{self|A}$ to penalize highly similar attributes for enhancing attribute differences, as:

$$\mathcal{L}_{self|A} = -\frac{1}{\mathbf{D}}\log\frac{\text{tr}\big(\exp(\mathbf{S}_A \odot \mathbf{S}_A/\tau)\big)}{\sum \mathbf{S}_A}, \quad (7)$$

where $\sum \mathbf{S}_A$ notes the sum of all elements of the matrix $\mathbf{S}$.

Graph-level node self-contrast loss $\mathcal{L}_{self|N}$ is consistent with the above description. We use the graph kernel method, e.g., SP, GK, WL, LT to calculate graph similarity, treating each subgraph as a node and generating an adjacent matrix $\bar{\mathbf{A}}$ to pull positive sample pairs in and negative sample pairs away. Then, The graph-level node correlation matrix $\mathbf{S}_{N_G}$ is calculated as:

$$\mathbf{S}_{N_G} = \frac{(\widetilde{\mathbf{Z}})^\top(\widetilde{\mathbf{Z}})}{||\widetilde{\mathbf{Z}}||^2}. \quad (8)$$

The optimization goals are as:

$$\mathcal{L}_{self|N} = -\frac{1}{N_G}\log\frac{\text{tr}\big(\bar{\mathbf{A}}\exp(\mathbf{S}_{N_G} \odot \mathbf{S}_{N_G}/\tau)\big)}{\sum \mathbf{S}_{N_G}}, \quad (9)$$

Meanwhile, we also introduce a comparative KL loss $\mathcal{L}_{KL}$ as:

$$\mathcal{L}_{KL} = \sum_{i=1}^{n}\sum_{k=1}^{K} \mathbf{P}_{ik}\log\frac{\mathbf{P}_{ik}}{\mathbf{Q}_{ik}}, \quad (10)$$

where $\mathbf{Q}$ is soft assignment distribution generated by final fusion graph-level embedding $\widetilde{\mathbf{Z}}$, and $\mathbf{P}$ as the target distribution is the sharpen distribution of $\mathbf{Q}$. In this way, DBGCN emphasizes high-confidence samples while reducing the impact of noisy or uncertain data, thereby enhancing the separability of clusters. Furthermore, $\mathcal{L}_{KL}$ facilitates the alignment of the fused embedding $\widetilde{\mathbf{Z}}$ with the target distribution, leading to more compact and well-separated clusters. This loss also promotes the effective integration of multi-view information, ensuring that the fused representation captures global features while preserving local consistency. Finally, the overall optimization goal is as:

$$\mathcal{L} = \alpha \times \mathcal{L}_{self} + \beta \times \mathcal{L}_{KL} \quad (11)$$

IV. Experiments

A. Benchmark Datasets

We evaluate COLLAB represents scientific collaboration networks, where nodes correspond to authors and edges denote co-authorships. The ground truth clusters are derived from research communities or predefined scientific fields. IMDB-BINARY contains movie collaboration networks, where nodes correspond to actors and edges represent co-appearances in the same movie. The ground truth labels distinguish movies by genre or production attributes. BZR consists of chemical compound graphs, where nodes represent atoms and edges correspond to chemical bonds. Ground truth clusters are determined based on molecular functional groups or known bioactivity classes. COX2 focuses on protein-protein interaction networks, where nodes are proteins and edges represent physical interactions. Ground truth labels follow protein families or functional classifications. Letter-low serves as a benchmark in computer vision, where nodes represent strokes in handwritten letters, and edges capture spatial relationships. The ground truth is based on character classes. The specific parameters are shown in Table I.

TABLE I: Detailed information of the datasets used in the experiment.

Dataset Name	Graph Classes	Average nodes	Average edges	Node Attr	Graphs	Node Classes	Domain
COX2 [30], [31]	2	41.22	43.45	+(3)	467	8	Small molecules
BZR [32]	2	35.75	38.36	+(3)	405	10	Small molecules
IMDB-BINARY [33]	2	17.93	19.39	-	188	-	Social networks
COLLAB [34]	3	74.49	2457.78	-	5000	-	Social networks
Letter-low [35]	15	4.68	3.13	+(2)	2250	18	Computer vision
Synthie [36]	4	95	172.9	+(15)	400	-	Synthie

TABLE II: The clustering results (expressed as mean ± standard deviation) on the COX2, BZR, and IMDB datasets are reported in percentages. **Bold** and underlined figures represent the highest and second-highest performances, respectively.

Method	COX2				BZR				IMDB-BINARY			
	ACC	NMI	ARI	F1	ACC	NMI	ARI	F1	ACC	NMI	ARI	F1
RW	51.3±0.0	0.7±0.0	0.0±0.0	37.5±0.0	60.6±0.0	0.0±0.0	0.0±0.0	24.6±0.0	51.3±0.0	0.1±0.0	0.0±0.0	24.4±1.2
SP	52.0±0.0	0.1±0.0	0.0±0.0	37.2±0.0	79.5±0.0	4.1±0.0	3.9±0.0	26.5±0.0	53.9±0.0	6.6±0.0	0.1±0.0	17.6±0.1
WL	50.5±0.0	0.1±0.0	0.0±0.0	32.1±0.0	65.5±0.0	0.0±0.0	0.0±0.0	19.9±0.1	51.2±0.0	0.7±0.0	0.6±0.0	26.3±0.2
LT	77.5±0.6	0.2±0.0	0.1±0.0	55.5±0.8	78.3±0.4	0.7±0.3	1.1±1.0	26.9±0.3	51.2±0.0	1.6±0.0	0.1±0.0	23.8±0.0
InfoGraph	56.4±3.2	3.3±0.6	0.2±0.0	37.1±2.6	63.6±0.4	1.6±0.3	2.4±1.0	33.4±0.2	54.7±0.0	4.7±0.1	0.9±0.0	36.5±1.2
GraphCL	68.8±0.6	1.0±0.2	0.4±0.5	44.2±1.8	72.8±4.0	1.0±0.8	3.4±1.0	38.1±0.7	57.6±0.0	5.1±0.2	2.7±0.0	38.8±0.9
JOAO	70.5±2.0	1.2±0.3	0.5±0.4	38.4±0.9	72.6±0.0	2.7±1.4	5.6±3.7	42.1±1.1	50.4±0.0	0.2±0.0	0.0±0.0	32.3±2.1
GFW	57.6±4.1	1.5±0.1	2.1±1.8	39.2±0.0	52.7±0.8	3.3±1.1	0.0±0.0	26.4±0.9	56.9±2.6	0.6±1.0	2.1±1.3	40.8±1.0
GLCC	77.3±0.0	0.1±0.3	0.0±0.0	42.1±0.0	63.6±0.0	1.1±0.0	1.1±3.4	42.6±2.5	66.5±0.0	8.1±0.0	10.6±0.0	52.9±1.2
UDGC	74.6±1.8	0.5±1.1	1.4±2.2	42.2±1.5	58.9±2.1	0.7±0.1	0.9±0.0	33.3±0.2	68.7±0.2	10.4±1.3	3.5±2.3	46.9±2.5
DGLC	78.3±0.2	2.3±0.1	6.7±3.4	66.3±2.1	80.9±0.6	9.8±0.9	20.5±1.8	75.5±2.6	66.2±0.2	8.9±0.5	4.4±1.4	53.6±3.3
OURS	**81.2±0.3**	**3.8±0.5**	**8.4±0.0**	**77.0±1.7**	**82.4±1.6**	**10.7±0.5**	**22.2±1.3**	**76.8±1.6**	**69.2±0.8**	**11.1±0.0**	**13.4±0.2**	**56.7±1.2**

TABLE III: The clustering results (expressed as mean ± standard deviation) on the COLLAB, Letter, and Synthie datasets are reported in percentages. **Bold** and underlined figures represent the highest and second-highest performances, respectively.

Method	COLLAB				Letter-Low				Synthie			
	ACC	NMI	ARI	F1	ACC	NMI	ARI	F1	ACC	NMI	ARI	F1
RW	N/A	N/A	N/A	N/A	12.6±0.0	10.5±0.0	8.9±0.0	9.7±0.0	23.4±0.0	10.7±0.0	13.2±0.0	19.6±0.0
SP	48.7±0.0	17.9±0.0	13.9±0.0	36.5±0.0	12.2±0.0	11.8±0.0	10.2±0.0	8.6±0.0	22.5±0.0	17.1±0.0	13.4±0.0	23.8±0.0
WL	53.2±0.0	2.0±0.0	0.6±0.0	48.3±0.0	10.4±0.0	8.9±0.0	7.5±0.0	7.5±0.0	21.9±0.0	8.6±0.0	12.8±0.0	20.0±0.0
LT	N/A	N/A	N/A	N/A	6.4±0.0	15.3±0.0	9.7±0.0	6.3±0.0	18.7±0.0	11.6±0.0	12.7±0.0	19.8±0.0
InfoGraph	56.9±1.8	14.2±3.0	6.6±2.7	39.1±2.6	16.8±0.1	18.2±0.5	10.4±1.2	11.7±0.4	44.0±1.6	35.5±3.2	31.4±2.2	38.7±1.9
GraphCL	58.0±1.2	17.8±1.9	11.3±0.6	44.2±1.5	19.4±0.9	15.4±0.2	13.2±0.8	16.9±0.1	36.5±1.1	18.7±0.4	20.1±0.6	31.8±0.4
JOAO	58.3±1.5	18.7±2.7	10.5±0.9	40.4±0.4	15.9±0.5	15.9±3.1	15.6±0.1	14.4±1.5	50.4±0.0	26.7±1.3	21.5±1.2	32.3±2.1
GFW	57.6±0.3	15.6±0.3	8.9±1.2	39.4±3.0	20.3±0.5	16.7±0.6	12.0±0.2	18.8±0.3	48.8±1.3	26.1±1.7	22.2±1.5	35.8±0.9
GLCC	54.4±0.2	12.7±1.3	7.7±2.4	38.1±1.3	37.4±0.4	20.5±2.3	11.1±0.1	32.3±1.5	36.5±0.0	23.4±1.2	17.7±0.8	32.4±1.3
UDGC	51.7±1.1	13.5±1.8	8.6±2.6	34.3±1.9	36.9±0.5	23.6±0.8	12.3±0.3	30.5±1.4	52.5±0.2	56.9±1.3	38.5±1.0	44.2±0.9
DGLC	61.5±1.5	19.9±1.4	12.7±0.8	51.6±2.0	39.6±2.0	30.3±1.0	17.5±0.6	35.4±1.0	38.6±0.2	28.9±0.5	26.3±1.4	48.5±3.3
OURS	**63.3±0.5**	**23.7±0.2**	**14.1±0.2**	**55.7±0.3**	**40.8±1.4**	**42.5±1.2**	**22.6±1.3**	**39.6±1.1**	**54.4±0.6**	**58.8±0.3**	**40.2±0.7**	**52.3±0.8**

B. Baseline Methods

We compare DBGCN with eleven state-of-the-art baselines, which can be broadly classified into three categories including: i) Graph Kernel: RW [37], SP [38], WL [32], and LT [39]; ii) Unsupervised Graph Representation Learning: InfoGraph [40], GraphCL [41], JOAO [42]; iii) Graph-Level Clustering: GFW [11], GLCC [12], UDGC [13] and DGLC [14]. The baselines not mentioned above are introduced as follows:

- **InfoGraph.** InfoGraph to encode the transformed graph by using a GNN model and compare the encoding result with the original graph to maximize the similarity between them.
- **GraphCL.** GraphCL constructs local contrastive tasks and global contrastive tasks to maximize the similarity.
- **JOAO.** The key idea of JOAO is the introduction of a connection-based graph embedding optimization framework, in which the connection relationships between nodes are treated as a hypersphere in the embedding space.

Parameters Setting The experimental setup is as follows: we use 4 layers for both the GCN encoder and GIN encoder, with a feature dimension of 16. Training is conducted with a batch size of 256 for 100 epochs using the Adam optimizer. Evaluation metrics include Clustering Accuracy (ACC) [43], Normalized Mutual Information (NMI) [44], Adjusted Rand Index (ARI) [45], and F1 score, reported as the mean and standard deviation over 10 independent runs per dataset. The experiments are run on a Windows operating system with an NVIDIA GeForce RTX 4090 GPU.

C. Comparison Experiments

Based on the above experiment settings, the results are shown in Table II and III. For these clustering results, we

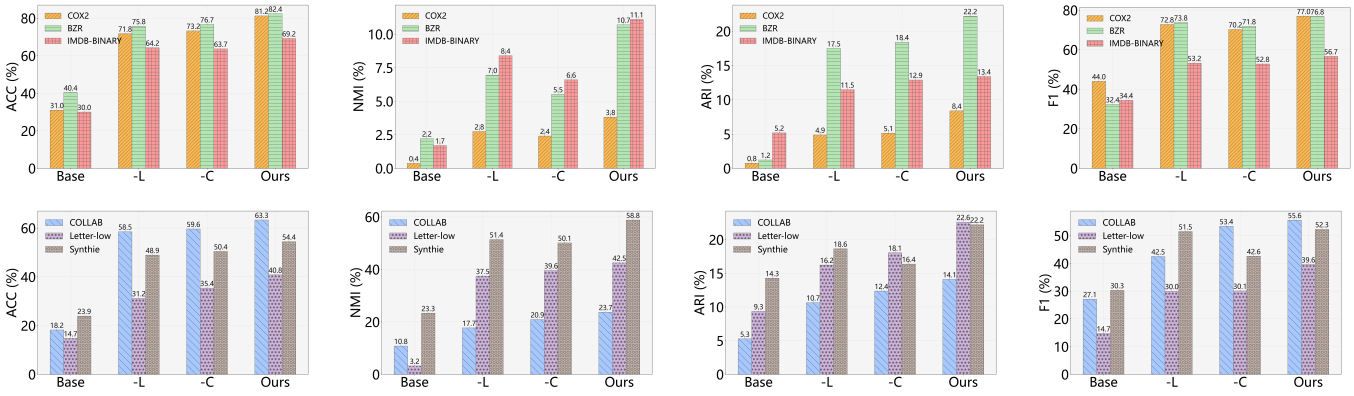

(a) ACC (b) NMI (c) ARI (d) F1

Fig. 2: Ablation study outcomes showing the impact of LHPM (-L) and MCFS (-C) on performance. The metrics include ACC, NMI, ARI, and F1 Score.

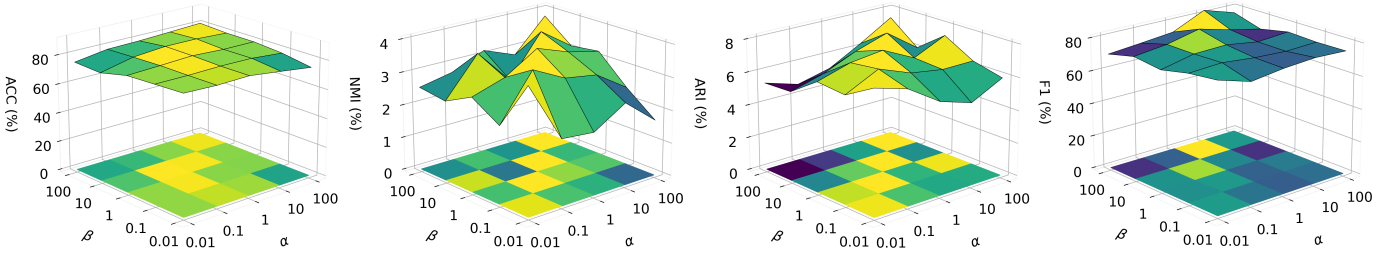

(a) ACC (b) NMI (c) ARI (d) F1

Fig. 3: The impact of α and β to the clustering performance on COX2. α and β changes in the range of [0.01, 100].

conclude several observations below.

- Compared to existing approaches, DBGCN outperforms them across all evaluation metrics, demonstrating its superior representation learning capability.
- Compared to traditional spectral clustering methods, our proposed approach demonstrates significant performance superiority. This advantage primarily arises from the fact that they rely solely on specific patterns and fail to adapt to evolving graph structures, thereby limiting their ability to generate cluster-friendly representations.
- Compared to existing state-of-the-art methods, our proposed approach significantly improves performance, particularly in terms of NMI and ARI. This enhancement is primarily due to MCFS, which employs contrastive learning to compress intra-cluster distances while increasing inter-cluster separation, leading to clearer graph-level clustering boundaries.
- In terms of adaptability, MCFS enhances graph-level features by preserving high-dimensional information while effectively removing noise, consistently delivering superior performance across a variety of graph types, including graphs with and without node attributes, as well as homogeneous and heterogeneous graphs.
- In terms of graph-level noise filtering, LHPM demonstrates strong performance on datasets with redundant node features by effectively filtering out low-value features at the graph level while preserving those with high clustering relevance. This selective feature retention process enhances the overall quality of node representations by prioritizing the most friendly clustering information of the data, thus optimizing the clustering process. Through this approach, LHPM improves the discriminative power and accuracy of the resulting graph-level representations.
- DBGCN exhibits robust performance across a range of datasets with varying types and classification quantities, highlighting its versatility and broad applicability.

D. Module Ablation Studies

We conduct ablation studies to evaluate the impact of enhancing the DBGCN approach by integrating additional components. Specifically, we test the effects of introducing LHPM (-L) and MCFS (-C) to the base network. When MCFS is not used, we choose the structure encoding as the input of the model. The results in Fig. 2 demonstrate:

- Incorporating LHPM significantly improved evaluation metrics, demonstrating its superiority in feature aggregation and information extraction. Even in the presence of substantial noise, LHPM effectively captured essential information while suppressing irrelevant features. Furthermore, in high-dimensional and complex graphs,

TABLE IV: Clustering performance with noise (MEAN ± STD). We add node attribute noise, graph structure noise, and mixed noise (node attribute noise and graph structure noise) to the two benchmark datasets, taking 0.1 and 0.2 as the interference rate. At the same time, we compare it with the GLCC model. R indicates the interference rate in the table.

R	Model	COX2						IMDB-BINARY					
		Attribute Noise		Structure Noise		Mixed Noise		Attribute Noise		Structure Noise		Mixed Noise	
		ACC	**NMI**	**ACC**	**NMI**	**ACC**	**NMI**	**ACC**	**NMI**	**ACC**	**NMI**	**ACC**	**NMI**
0.1	GLCC	70.3±2.3	0.1±0.0	67.4±0.9	0.0±0.0	62.1±1.7	0.0±0.1	58.4±2.3	3.7±1.6	59.3±2.0	4.4±0.6	56.6±1.5	4.0±0.4
	OURS	**80.9±2.3**	**3.2±0.3**	**80.1±0.0**	**3.5±0.5**	**80.0±0.8**	**11.5±0.3**	**69.1±0.7**	**11.8±0.4**	**67.3±0.9**	**9.4±1.2**	**67.7±0.8**	**8.6±0.3**
0.2	GLCC	70.0±2.3	0.0±0.0	58.4±1.9	0.1±0.0	56.7±1.1	0.0±0.0	59.5±1.7	5.6±0.3	58.4±1.9	5.2±0.2	56.7±1.1	4.9±0.5
	OURS	**80.1±1.3**	**3.0±0.0**	**79.6±1.5**	**3.1±2.7**	**79.4±1.8**	**3.4±0.0**	**69.4±1.3**	**3.0±0.0**	**66.6±1.5**	**9.0±1.1**	**64.8±1.2**	**8.8±0.4**
R	**Model**	**BZR**						**Letter-low**					
0.1	GLCC	60.3±1.9	0.9±0.0	58.5±1.6	0.6±0.0	55.3±1.2	0.6±0.1	28.7±2.2	18.6±1.9	32.2±1.0	20.2±0.7	17.5±1.9	18.3±1.1
	OURS	**80.5±1.2**	**9.1±0.2**	**78.9±1.8**	**9.3±0.6**	**78.7±1.9**	**9.1±0.3**	**36.2±0.3**	**32.5±0.8**	**38.1±0.2**	**35.6±0.2**	**34.3±0.4**	**36.7±0.3**
0.2	GLCC	55.6±2.7	0.7±0.0	53.4±2.1	0.9±0.1	54.2±1.5	0.7±0.1	20.2±1.2	28.0±1.0	22.5±2.0	30.3±0.6	12.6±1.5	15.7±3.6
	OURS	**79.3±2.0**	**9.5±0.4**	**78.0±0.2**	**8.9±0.5**	**77.9±1.8**	**9.0±0.6**	**34.5±0.4**	**30.3±0.8**	**36.2±1.5**	**34.9±1.5**	**30.3±0.8**	**35.7±1.9**

it generated more discriminative graph-level representations, enhancing robustness and generalization.

- Compared to the baseline, the introduction of MCFS effectively leverages the complementary strengths of subspace and global information, optimizing graph-level representations through comparative methods. This enhancement improves graph-level embedding quality, significantly outperforming the baseline across various metrics.
- In datasets with missing attributes e.g., COLLAB and Letter-low, the absence of the fusion mechanism in MCFS has a negligible impact on the performance. The main reason for its lower performance compared to our proposed method is the lack of a contrastive mechanism to optimize the representation.
- The evaluations show that the combination of the two promotes each other and reaches peak performance.

E. Comparative Ablation

In order further to explore the impact of using different pooling variants on experimental performance, we select several advanced pooling methods: diffpool and attention pooling. The experimental results are shown in Fig. **??**, and the following conclusions are obtained

F. Hyper-parameter Analysis

The DBGCN includes two hyperparameters, α and β, to balance self-contrast loss and KL loss. The results, as shown in Fig. 3, illustrate that when the loss ratio between α and β is 1:1, the two losses effectively complement each other, leading to optimal performance. Additionally, the performance metrics, including NMI and ARI, demonstrate a highlight sensitivity to changes in α, whereas ACC and F1 are predominantly influenced by the ratio between α and β. This is attributed to our graph-level comparison mechanism, which brings positive pairs closer together and pushes negative pairs apart, improving the cohesion of clusters. Notably, even under extreme ratios, our model consistently outperforms existing state-of-the-art methods in terms of both ACC and F1.

G. Complexity Analysis

We analyze the time complexity of each component in DBGCN. For the encoder components, both GCN and GIN have a complexity of $O(L_e nd^2 + mdL_e)$, where L_e is the number of layers, n is the number of nodes, m is the number of the edges, and d is the feature dimension. The complexity of the fusion module with MLP is $O(nd^2)$. For the hierarchical pooling process, the complexity is $O(L_p n_g d^2)$, where L_p is the number of refinement layers and n_g is the sum of graphs. About the loss, $\mathcal{L}_{self}$ has a complexity of $O(n_g d)$, $\mathcal{L}_{KL}$ has a complexity of $O(n_g)$.

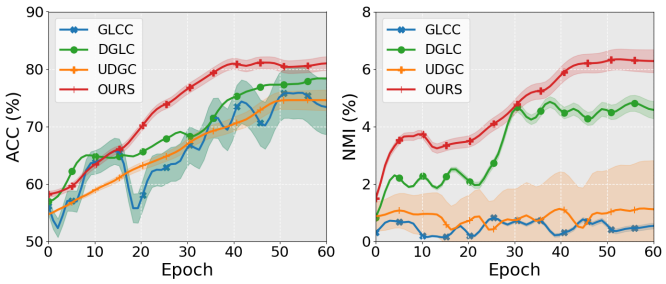

Fig. 4: Convergence analysis of DBGCN: evaluating the stability of ACC and NMI across multiple experiments with 60 training epochs on COX2 benchmark.

H. The Performance Under Noise

To comprehensively validate the effectiveness of our DBGCN framework in mitigating various noises, we introduce noise into both node attributes and graph structures. Node attribute noise is introduced by randomizing node features, whereas graph structure noise is incorporated through random edge perturbations. The experimental results, presented in the Table IV, lead to the following conclusions:

- Adding noise has a minimal impact (a drop of $< 2\%$ in ACC) on our network, which consistently outperforms existing models. This can be attributed to the multiple noise filters that suppress the propagation of unfriendly-clustering information.

TABLE V: T-test results of DGLC and Ours on four datasets. To alleviate the adverse influence of randomness, we repeat each experiment 10 times and record their performance for t-test comparison.

Dataset	Algorithm	Performance										P-vaule
COX2	DGLC	78.1	78.2	78.3	78.1	78.3	78.4	78.2	78.5	78.2	78.3	<0.05
	Ours	81.4	80.9	81.22	81.8	81.0	81.5	81.3	80.9	81.2	81.69	
IMDB-B	DGLC	65.9	66.5	66.1	66.2	65.9	66.0	66.2	66.2	66.1	66.2	<0.05
	Ours	67.6	68.2	70.1	69.6	69.1	68.7	68.3	70.0	69.7	67.3	
COLLAB	DGLC	61.1	62.0	60.4	65.2	61.2	61.8	60.0	59.3	59.5	62.7	<0.05
	Ours	62.9	63.5	63.5	64.5	63.9	62.9	64.1	64.5	63.4	62.8	
Letter-Low	DGLC	38.1	40.6	40.9	39.2	39.9	43.3	38.0	41.0	38.2	38.4	<0.05
	Ours	40.7	40.3	42.3	41.6	40.0	40.8	40.2	41.6	40.2	41.8	

- Since the novel pooling mechanism enhances robustness to mixed noise, our model effectively mitigates noise amplification compared to GLCC.
- The influence of node attribute noise is generally less significant than that of structural features in most datasets, as the optimization of graph-level representations is primarily driven by structural information; moreover, some datasets are driven mainly by attribute features. Therefore, the impact of adding different noise varies and lacks consistency across datasets.
- On some datasets, adding noise actually slightly improves NMI and ARI. This is attributed to the fact that an appropriate amount of noise increases the diversity of the data, which help the model better distinguish different categories.

I. Convergence Analysis

To assess the stability of DBGCN, we perform several experiments using random seeds ranging from 1 to 10 and compute the average and standard deviation of the results. Fig. 4 shows the curves of the average test accuracy along with the standard deviation during training across five runs, comparing DBGCN with the advanced GLCC, UDGC, and DGLC methods. It is clear that DBGCN not only achieves the highest average test accuracy and converges more quickly than the other methods but also exhibits a smaller variance, further substantiating the effectiveness and stability of our proposed enhancement method in feature alignment, noise filtering, and graph-level discrimination.

J. Visualize Results

In order to explore the impact of using different pooling variants on experimental performance, we select several advanced pooling methods diffpool and attention pooling. The experimental results are shown in Figure 1, and the following conclusions are obtained

K. T-Test

To validate the effectiveness of our method, we conducted hypothesis testing to systematically evaluate the differences between our approach and existing advanced methods, ensuring that the observed improvements are statistically significant. Specifically, we formulated a null hypothesis, which assumes no significant difference between the two methods, and an alternative hypothesis, which posits that our method outperforms the DGLC method. The experimental results, presented in Table V, show a p-value less than 0.05, which leads to the rejection of the null hypothesis and the acceptance of the alternative hypothesis. Consequently, our method significantly enhances performance.

V. Conclusion

In this paper, we propose a novel clustering framework specifically designed for graph-level data, termed DBGCN, which effectively extracts high-confidence graph-level features, thereby enhancing clustering performance. In DBGCN, MCFS filters out interference information in high-dimensional space. LHPM gradually refines context features and produces enriched graph-level representations. DBGCN exhibits exceptional efficacy in capturing key features and reducing redundancy, even in complex graph structures with high noise levels. The experiment results indicate that DBGCN consistently surpasses state-of-the-art methods across six benchmark datasets. Notably, the approach exhibits superior robustness when applied to datasets of varying scales and intricacies, making it particularly effective in clustering tasks involving intricate, heterogeneous graphs. In the future, we plan to refine its architecture and applications to overcome specific limitations encountered in specialized environments.

VI. Acknowledgment

This work is supported by the Natural Science Foundation of Hainan University (No. XJ2400009401). Thanks to Associate Researcher Wenxuan Tu, the correspondent of this paper.

References

[1] Y. Wei, H. Guo, Z. Ge, and Z. Yang, "Graph attention-based deep embedded clustering for speaker diarization," *Speech Communication*, vol. 155, p. 102991, 2023.

[2] S. Qin, T. Jiang, S. Wu, N. Wang, and X. Zhao, "Graph convolution-based deep clustering for speech separation," *IEEE Access*, vol. 8, pp. 82 571–82 580, 2020.

[3] S. Takahashi, S. Sakti, and S. Nakamura, "Unsupervised neural-based graph clustering for variable-length speech representation discovery of zero-resource languages." in *Interspeech*, 2021, pp. 1559–1563.

[4] T. J. Loftus, B. Shickel, J. A. Balch, P. J. Tighe, K. L. Abbott, B. Fazzone, E. M. Anderson, J. Rozowsky, T. Ozrazgat-Baslanti, Y. Ren *et al.*, "Phenotype clustering in health care: a narrative review for clinicians," *Frontiers in artificial intelligence*, vol. 5, p. 842306, 2022.

[5] W.-C. Yang, J.-P. Lai, Y.-H. Liu, Y.-L. Lin, H.-P. Hou, and P.-F. Pai, "Using medical data and clustering techniques for a smart healthcare system," *Electronics*, vol. 13, no. 1, p. 140, 2023.

[6] C. X. Gao, D. Dwyer, Y. Zhu, C. L. Smith, L. Du, K. M. Filia, J. Bayer, J. M. Menssink, T. Wang, C. Bergmeir *et al.*, "An overview of clustering methods with guidelines for application in mental health research," *Psychiatry Research*, vol. 327, p. 115265, 2023.

[7] J. Ferris, L. K. Fiedeldey, B. Kim, F. Clemens, M. A. Irvine, S. H. Hosseini, K. Smolina, and A. Wister, "Protocol: Systematic review and meta-analysis of disease clustering in multimorbidity: a study protocol," *BMJ open*, vol. 13, no. 12, 2023.

[8] W. Zhao, W. Zou, and J. J. Chen, "Topic modeling for cluster analysis of large biological and medical datasets," in *BMC bioinformatics*, vol. 15. Springer, 2014, pp. 1–11.

[9] U. Von Luxburg, "A tutorial on spectral clustering," *Statistics and computing*, vol. 17, pp. 395–416, 2007.

[10] R. Vidal, "Subspace clustering," *IEEE Signal Processing Magazine*, vol. 28, no. 2, pp. 52–68, 2011.

[11] H. Xu, J. Liu, D. Luo, and L. Carin, "Representing graphs via gromov-wasserstein factorization," *IEEE Transactions on Pattern Analysis and Machine Intelligence*, vol. 45, no. 1, pp. 999–1016, 2022.

[12] W. Ju, Y. Gu, B. Chen, G. Sun, Y. Qin, X. Liu, X. Luo, and M. Zhang, "Glcc: A general framework for graph-level clustering," in *Proceedings of the AAAI conference on artificial intelligence*, vol. 37, no. 4, 2023, pp. 4391–4399.

[13] M. Hu, C. Chen, W. Liu, X. Zhang, X. Liao, and X. Zheng, "Learning uniform clusters on hypersphere for deep graph-level clustering," *arXiv e-prints*, pp. arXiv–2311, 2023.

[14] J. Cai, Y. Han, W. Guo, and J. Fan, "Deep graph-level clustering using pseudo-label-guided mutual information maximization network," *Neural Computing and Applications*, vol. 36, no. 16, pp. 9551–9566, 2024.

[15] M. Niepert, M. Ahmed, and K. Kutzkov, "Learning convolutional neural networks for graphs," in *International conference on machine learning*. PMLR, 2016, pp. 2014–2023.

[16] J. Lee, H. Lee, S. Seo, and J. Kim, "Graph attention pooling," in *Proceedings of the 33rd Conference on Neural Information Processing Systems (NeurIPS)*, 2019. [Online]. Available: https://arxiv.org/abs/1905.12265

[17] L. Zhang, X. Zhang, Y. Zhang, X. Wang, and H. Hu, "Attention-based graph pooling," in *Proceedings of the International Conference on Learning Representations (ICLR)*, 2020. [Online]. Available: https://openreview.net/forum?id=H1g2B9rKDH

[18] Y. Lv, Z. Tian, Z. Xie, and Y. Song, "Multi-scale graph pooling approach with adaptive key subgraph for graph representations," in *Proceedings of the 32nd ACM International Conference on Information and Knowledge Management*, 2023, pp. 1736–1745.

[19] J. Lee, I. Lee, and J. Kang, "Self-attention graph pooling," in *International conference on machine learning*. pmlr, 2019, pp. 3734–3743.

[20] Z. Ying, J. You, C. Morris, X. Ren, W. Hamilton, and J. Leskovec, "Hierarchical graph representation learning with differentiable pooling," *Advances in neural information processing systems*, vol. 31, 2018.

[21] M. Defferrard, X. Bresson, and P. Vandergheynst, "Convolutional neural networks on graphs with fast localized spectral filtering," *Advances in neural information processing systems*, vol. 29, 2016.

[22] W. H. L. Pinaya, S. Vieira, R. Garcia-Dias, and A. Mechelli, "Autoencoders," in *Machine learning*. Elsevier, 2020, pp. 193–208.

[23] D. Bo, X. Wang, C. Shi, M. Zhu, E. Lu, and P. Cui, "Structural deep clustering network," in *Proceedings of the web conference 2020*, 2020, pp. 1400–1410.

[24] W. Tu, S. Zhou, X. Liu, X. Guo, Z. Cai, E. Zhu, and J. Cheng, "Deep fusion clustering network," in *Proceedings of the AAAI Conference on Artificial Intelligence*, vol. 35, no. 11, 2021, pp. 9978–9987.

[25] C. Wang, S. Pan, R. Hu, G. Long, J. Jiang, and C. Zhang, "Attributed graph clustering: A deep attentional embedding approach," in *IJCAI*, 7 2019, pp. 3670–3676. [Online]. Available: https://doi.org/10.24963/ijcai.2019/509

[26] X. Peng, J. Cheng, X. Tang, J. Liu, and J. Wu, "Dual contrastive learning network for graph clustering," *IEEE Transactions on Neural Networks and Learning Systems*, 2023.

[27] K. Xu, W. Hu, J. Leskovec, and S. Jegelka, "How powerful are graph neural networks?" *arXiv preprint arXiv:1810.00826*, 2018.

[28] I. O. Tolstikhin, N. Houlsby, A. Kolesnikov, L. Beyer, X. Zhai, T. Unterthiner, J. Yung, A. Steiner, D. Keysers, J. Uszkoreit *et al.*, "Mlp-mixer: An all-mlp architecture for vision," *Advances in neural information processing systems*, vol. 34, pp. 24 261–24 272, 2021.

[29] Y. Tan, Y. Liu, G. Long, J. Jiang, Q. Lu, and C. Zhang, "Federated learning on non-iid graphs via structural knowledge sharing," in *Proceedings of the AAAI conference on artificial intelligence*, vol. 37, no. 8, 2023, pp. 9953–9961.

[30] K. A. W. J. C. C. R. et al., "Graph classification with attention mechanisms," in *Proceedings of the International Conference on Machine Learning (ICML)*, 2020.

[31] J. J. Sutherland, L. A. O'brien, and D. F. Weaver, "Spline-fitting with a genetic algorithm: A method for developing classification structure-activity relationships," *Journal of chemical information and computer sciences*, vol. 43, no. 6, pp. 1906–1915, 2003.

[32] N. Shervashidze, P. Schweitzer, E. J. Van Leeuwen, K. Mehlhorn, and K. M. Borgwardt, "Weisfeiler-lehman graph kernels." *Journal of Machine Learning Research*, vol. 12, no. 9, 2011.

[33] P. Yanardag and S. V. N. Vishwanathan, "Deep graph kernels," in *Proceedings of the 21th ACM SIGKDD International Conference on Knowledge Discovery and Data Mining (KDD)*, 2015, pp. 1365–1374.

[34] A. et al., "Graph neural networks for learning with graphs," *IEEE Transactions on Neural Networks and Learning Systems*, vol. 32, no. 1, pp. 4–19, 2021.

[35] G. Defferrard, M. Simonnet, and L. F. A. D. A. et al., "Convolutional neural networks on graphs with fast localized spectral filtering," in *Advances in Neural Information Processing Systems (NeurIPS)*, 2016.

[36] C. Morris, N. M. Kriege, K. Kersting, and P. Mutzel, "Faster kernels for graphs with continuous attributes via hashing," in *2016 IEEE 16th International Conference on Data Mining (ICDM)*. IEEE, 2016, pp. 1095–1100.

[37] K. M. Borgwardt and H.-P. Kriegel, "Shortest-path kernels on graphs," in *Proceedings of the Fifth IEEE International Conference on Data Mining (ICDM)*. IEEE, 2005, pp. 74–81.

[38] K. Borgwardt and H. P. Kriegel, "Short paper: Graph kernels," in *Proceedings of the Fifth IEEE International Conference on Data Mining (ICDM)*, 2005, pp. 28–35.

[39] F. Johansson, V. Jethava, D. Dubhashi, and C. Bhattacharyya, "Global graph kernels using geometric embeddings," in *International Conference on Machine Learning*. PMLR, 2014, pp. 694–702.

[40] F.-Y. Sun, J. Hoffmann, V. Verma, and J. Tang, "Infograph: Unsupervised and semi-supervised graph-level representation learning via mutual information maximization," *arXiv preprint arXiv:1908.01000*, 2019.

[41] Y. You, T. Chen, Y. Sui, T. Chen, Z. Wang, and Y. Shen, "Graph contrastive learning with augmentations," *Advances in neural information processing systems*, vol. 33, pp. 5812–5823, 2020.

[42] J. e. a. You, "Joao: A joint learning framework for graph neural networks," in *Proceedings of the 38th International Conference on Machine Learning (ICML)*, 2021, pp. 1953–1963.

[43] W. Tu, R. Guan, S. Zhou, C. Ma, X. Peng, Z. Cai, Z. Liu, J. Cheng, and X. Liu, "Attribute-missing graph clustering network," in *Proceedings of the AAAI Conference on Artificial Intelligence*, vol. 38, no. 14, 2024, pp. 15 392–15 401.

[44] S. Pan, R. Hu, S.-f. Fung, G. Long, J. Jiang, and C. Zhang, "Learning graph embedding with adversarial training methods," *IEEE transactions on cybernetics*, vol. 50, no. 6, pp. 2475–2487, 2019.

[45] J. Liu, X. Liu, Y. Yang, X. Guo, M. Kloft, and L. He, "Multiview subspace clustering via co-training robust data representation," *IEEE Transactions on Neural Networks and Learning Systems*, vol. 33, no. 10, pp. 5177–5189, 2021.

[46] L. Van der Maaten and G. Hinton, "Visualizing data using t-sne," *Journal of Machine Learning Research*, vol. 9, no. Nov, pp. 2579–2605, 2008.